Heat Generation during the Firing of a Capacitor Based Railgun System

Andrew N. Smith

Mechanical Engineering Department
U.S. Naval Academy

Benjamin T. McGlasson and Jack S. Bernardes

Naval Surface Warfare Center
Dahlgren Division

Abstract— Railguns use a high-current, high-energy electrical pulse to accelerate projectiles to hypersonic velocities. Pulse forming networks that employ capacitors as the energy store are typically used to shape the required electrical pulse. A significant fraction of the stored energy (25 – 40% in large caliber railguns) is converted to projectile kinetic energy during launch. After the projectile exits the launcher, the balance of the energy has either been dissipated as heat in the circuit components or is stored in system inductance. If an energy recovery scheme is not employed, the inductor energy will also be dissipated in the resistance of the active circuit components. A circuit analysis has been performed in order to calculate the current profile from the PFN. A higher fidelity solution was achieved by accounting for the temperature dependent resistance of the rails. This information along with individual component resistance and inductance was used to calculate the distribution of energy subsequent to a single pulse. Detailed component heating information is important when considering the overall thermal management of the system. Once this information has been obtained, the components that require external cooling can be identified, and an appropriate thermal management system can in turn be designed.

I. INTRODUCTION

The electromagnetic railgun has been proposed as a weapon that could enable the US Navy to conduct long-range surface fire support missions [1]. Several

Report Documentation Page

Form Approved
OMB No. 0704-0188

1. REPORT DATE	2. REPORT TYPE	3. DATES COVERED
2006		**00-00-2006 to 00-00-2006**

4. TITLE AND SUBTITLE	5a. CONTRACT NUMBER
Heat Generation During the Firing of a Capacitor Based Railgun System	5b. GRANT NUMBER
	5c. PROGRAM ELEMENT NUMBER
6. AUTHOR(S)	5d. PROJECT NUMBER
	5e. TASK NUMBER
	5f. WORK UNIT NUMBER
7. PERFORMING ORGANIZATION NAME(S) AND ADDRESS(ES) **U.S. Naval Academy,Mechanical Engineering Department,Annapolis,MD,21402-5000**	8. PERFORMING ORGANIZATION REPORT NUMBER
9. SPONSORING/MONITORING AGENCY NAME(S) AND ADDRESS(ES)	10. SPONSOR/MONITOR'S ACRONYM(S)
	11. SPONSOR/MONITOR'S REPORT NUMBER(S)

12. DISTRIBUTION/AVAILABILITY STATEMENT
Approved for public release; distribution unlimited

13. SUPPLEMENTARY NOTES
Presented at the 13th International Symposium on Electromagnetic Launch Technology (EML), Held May 22 - 25, 2006 in Potsdam, Brandenburg, Germany Copyright 2006 IEEE. Published in the Proceedings, http://emlsymposium.org/archive.html#

14. ABSTRACT

15. SUBJECT TERMS

16. SECURITY CLASSIFICATION OF:			17. LIMITATION OF ABSTRACT	18. NUMBER OF PAGES	19a. NAME OF RESPONSIBLE PERSON
a. REPORT	b. ABSTRACT	c. THIS PAGE			
unclassified	**unclassified**	**unclassified**	**Same as Report (SAR)**	**9**	

investigations have been published to date that examine the capacitor based Pulse Forming Network (PFN) that would be required [2]. These investigations have typically focused on determining the total energy required in order to achieve the desired launch velocity. In many cases the individual resistance of several components have been combined into a total effective resistance. Bernardes et al. examined a capacitor based system that would be used to launch a 20 kg launch mass at 2500 m/s velocity [2]. Pitman et al. [3] used equations developed by Parker et al. [4] to simulate a capacitor based system by solving the governing equations using a Runge Kutta method. This investigation will use a similar approach however the system of equations has been solved using a second order finite difference method.

The most complicated component in the system is the launcher itself. The resistance of the launcher changes with time as the projectile physically moves down the barrel and the magnetic field diffuses into the rail. Several investigations have been performed using an analytical approach [5], segmented rail with an effective height [6]-[7], segmented rails where the magnetic field diffuses into multiple surfaces [8], and full three dimensional simulations of the launcher [9]. In this paper, an effective height model is used to simulate the transient rail resistance based on the method presented by Parker et al. [7]. These calculations were performed concurrently with the solution of the PFN in order to account for mutual effects.

II. CIRCUIT MODEL

In order to determine the heat generation in each of the components of the PFN, the entire circuit had to be modeled. The specific circuit that was modeled in this investigation is shown in Figure 1 and is based on the requirements for the notional naval railgun. Each module is triggered by an array of thyristors. An array of crowbar diodes prevents the circuit current from ringing. The following rules were implemented in the circuit code: (1) the diode is not included in the circuit until after the capacitor has discharged; (2) once the capacitor has fully discharged the diode prevents that capacitor from recharging and thereby removes the thyristor, bus bar and capacitor from the circuit. As shown in Figure 1, the individual resistances of the following components were included in the circuit: thyristors, diodes, bus bars, capacitors, inductors, launcher and the shunt. At the completion of each shot, all of the energy not transferred to the launch mass ultimately represents a resistive heat load in one of these components. It was assumed that the railgun muzzle shunt is purely resistive, and that no attempt was made at energy recovery.

The governing differential equation for the charge in the circuit is given by the following equation [4]:

$$L_s \sum_{i=1}^{n} \frac{\partial^2 q_i}{\partial t^2} + L_b \frac{\partial^2 q_b}{\partial t^2} + R_s \sum_{i=1}^{n} \frac{\partial q_i}{\partial t} + R_b \frac{\partial q_b}{\partial t} + \frac{q_b}{C_b} = 0 \qquad (1)$$

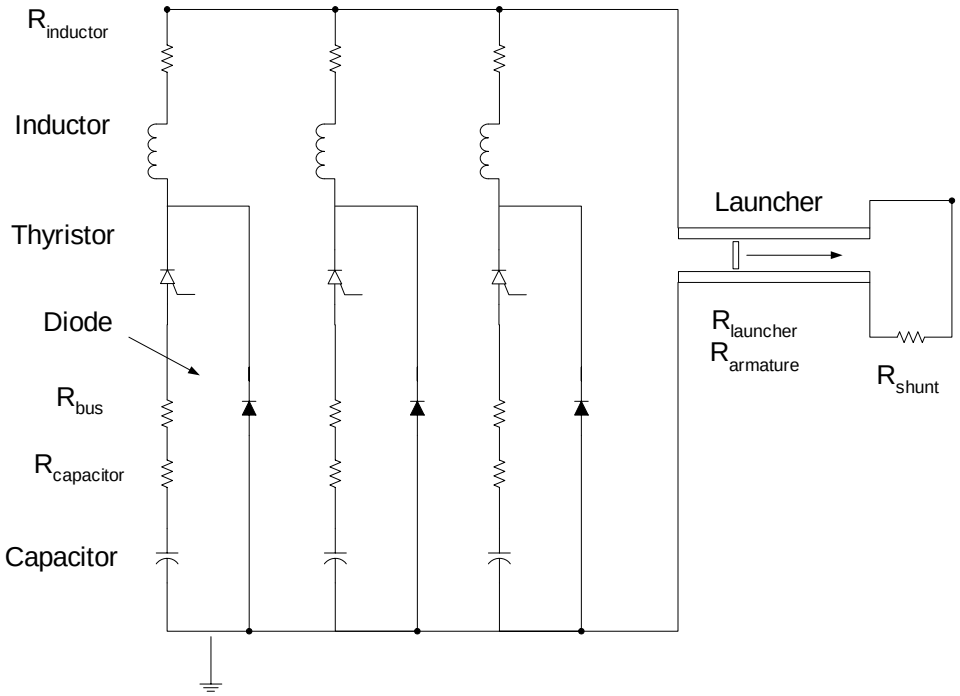

Figure 1. Capacitor-based PFN circuit that was used in the simulation. Although this figure only shows three banks, there are actually 35 individually triggered banks in the simulation.

where q_b is the charge of the capacitor for that bank and the summations are taken over the banks that are currently active. The subscript b denotes a particular bank and is used to identify the resistance, R; capacitance, C; and the inductance, L, of that bank. The subscript s refers to the system components that experience the total current summed over the individual banks. The resistance of the system, R_s, includes the resistance of the launcher, the resistance of the armature and the electromotive force on the armature.

Equation (1) is then be used to express the time varying charge of each active bank. Using a finite difference approach for the first and second order derivations, the system of differential equations can be solved simultaneously. Equation (2) shows the system of equations when there are three active banks, the size of the matrix grows as more banks are triggered.

$$\begin{bmatrix} \lambda_s+\lambda_{b,1}+\varepsilon_s+\varepsilon_{b,1} & \lambda_s+\varepsilon_s & \lambda_s+\varepsilon_s \\ \lambda_s+\varepsilon_s & \lambda_s+\lambda_{b,2}+\varepsilon_s+\varepsilon_{b,2} & \lambda_s+\varepsilon_s \\ \lambda_s+\varepsilon_s & \lambda_s+\varepsilon_s & \lambda_s+\lambda_{b,3}+\varepsilon_s+\varepsilon_{b,3} \end{bmatrix} \bullet \begin{bmatrix} q_{i+1,1} \\ q_{i+1,2} \\ q_{i+1,2} \end{bmatrix} =$$

$$\begin{bmatrix} \sum_{m=1}^{3}\lambda_s\left(2q_{i,m}-q_{i-1,m}\right)+\lambda_{b,1}\left(2q_{i,1}-q_{i-1,1}\right)+\sum_{m=1}^{3}\varepsilon_s q_{i,m}+\varepsilon_{b,2}q_{i,1}-\eta_{b,1}q_{i,1} \\ \sum_{m=1}^{3}\lambda_s\left(2q_{i,m}-q_{i-1,m}\right)+\lambda_{b,2}\left(2q_{i,2}-q_{i-1,2}\right)+\sum_{m=1}^{3}\varepsilon_s q_{i,m}+\varepsilon_{b,2}q_{i,2}-\eta_{b,2}q_{i,2} \\ \sum_{m=1}^{3}\lambda_s\left(2q_{i,m}-q_{i-1,m}\right)+\lambda_{b,3}\left(2q_{i,3}-q_{i-1,3}\right)+\sum_{m=1}^{3}\varepsilon_s q_{i,m}+\varepsilon_{b,3}q_{i,3}-\eta_{b,3}q_{i,3} \end{bmatrix} \quad (2)$$

where,

$$\lambda_{s,b} = \frac{L_{s,b}}{\Delta t^2} \tag{2a}$$

$$\varepsilon_{s,b} = \frac{R_{s,b}}{\Delta t} \tag{2b}$$

$$\eta_b = \frac{1}{C_b} \tag{2c}$$

The subscript *i* represents the time increment. The solution of this system of equations yields the charge in each capacitor banks at the future timestep *(i+1)*.

Figure 2 shows both the total current and the current of each individual bank during a simulated shot of a notional naval railgun. This simulation is based on launching a 20 kg mass to 2500 m/s using a 135mm square bore and a barrel length of 12 m. Table 1 provides the values of the key parameters used in this simulation. These values were typically based on the components to be used in the pulsed power system designed for installation at NSWC Dahlgren Division. It was assumed in this simulation that only the launcher resistance varied with time.

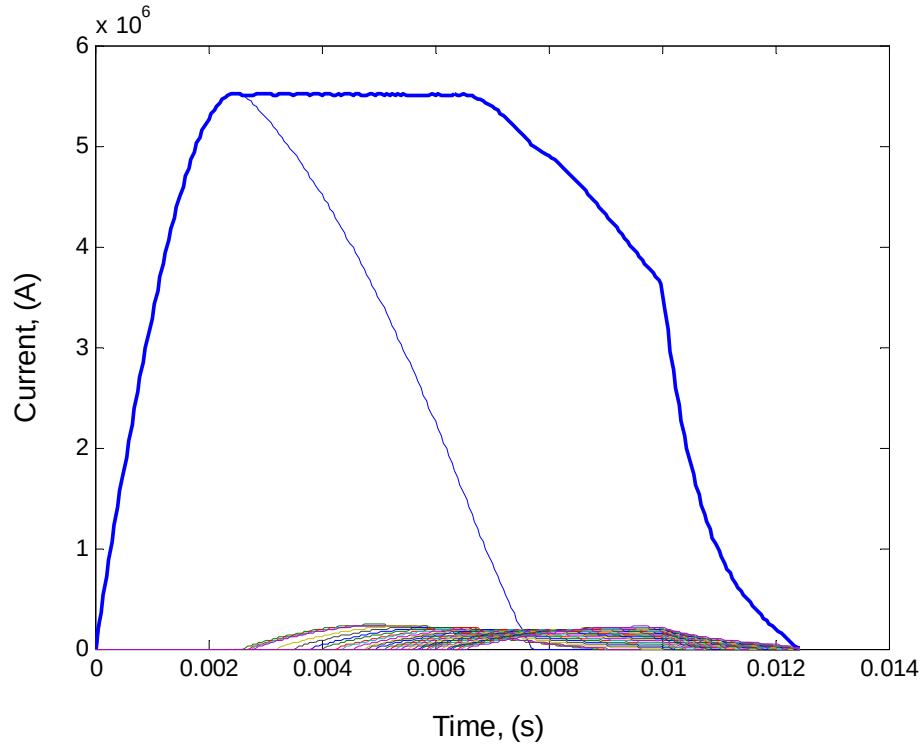

Figure 2. Total system current shown along with the current of each individual bank.

The resistance of the launcher was determined using an effective height model based on a 135mm square bore [6]-[8]. In order to calculate the effective height, the non-uniform surface current profile around the perimeter of the rail cross-section must be calculated. The effective height is then determined by equating the power dissipated in a surface layer on the perimeter of the rail, with a uniform current distribution on the front surface of a rail with an effective height [7]. Since the assumption was made that the current is uniform on the inside surface of the rail, a one dimensional finite difference approach was used to account for the diffusion of the magnetic field into the conductor. The temperature dependence of the resistivity of the rail material was taken into account, along with thermal diffusion occurring within the current pulse. It has been previously shown that it is necessary to account for thermal diffusion during the current pulse [8].

Table I. Properties of the circuit components used in the circuit model simulation.

Module Equivalent Values and Launcher Values	
Capacitor Charge Voltage (kV)	11.3
Equivalent Capacitance (mF)	49
Capacitor Resistance (u-ohms)	625
Crowbar Diode Resistance (u-ohms)	178
Thyristor Resistance (u-ohms)	183
Inductor Resistance (u-ohms)	350
Inductor Inductance (uH)	60
Bus Resistance (u-ohms)	63
Rail Resistivity (u-ohm-m)	0.017
Rail Effective Height (mm)	200
Rail Effective Width (mm)	42
Inductance Gradient (uH/m)	0.42
Muzzle Shunt Resistance (m-ohms)	10

III. HEAT GENERATION

Figure 3 shows the distribution of energy after the first shot. It is apparent that the majority of the energy is converted into the kinetic energy of the projectile. The resistive heating of the launcher is the third largest energy load. The effective height model is conservative; because, in order to apply an average current to a single surface, a higher average current is applied to a smaller total area. While the dissipated power for a surface layer is retained, this results in higher predicted temperatures than some areas of the rail would experience due to the lower thermal mass. Coupled with the temperature dependence of the electrical resistivity in the model, this increases the resistive load. The highly resistive shunt used in this simulation collects the majority of

the energy that remained in the magnetic fields of the launcher when the projectile departs. Although some form of energy recovery may be considered [10], great care will need to be taken such that these attempts do not increase the heat load throughout the rest of the system. It may prove to be easier to use a resistive shunt that has been designed with an effective cooling system. This will assure that the heat is dumped in an area where it is easily managed. The timestep used in the simulation was systematically reduced until the total energy after the shot in the form of heat and kinetic energy was within 0.1% of the initial energy stored in the capacitor banks.

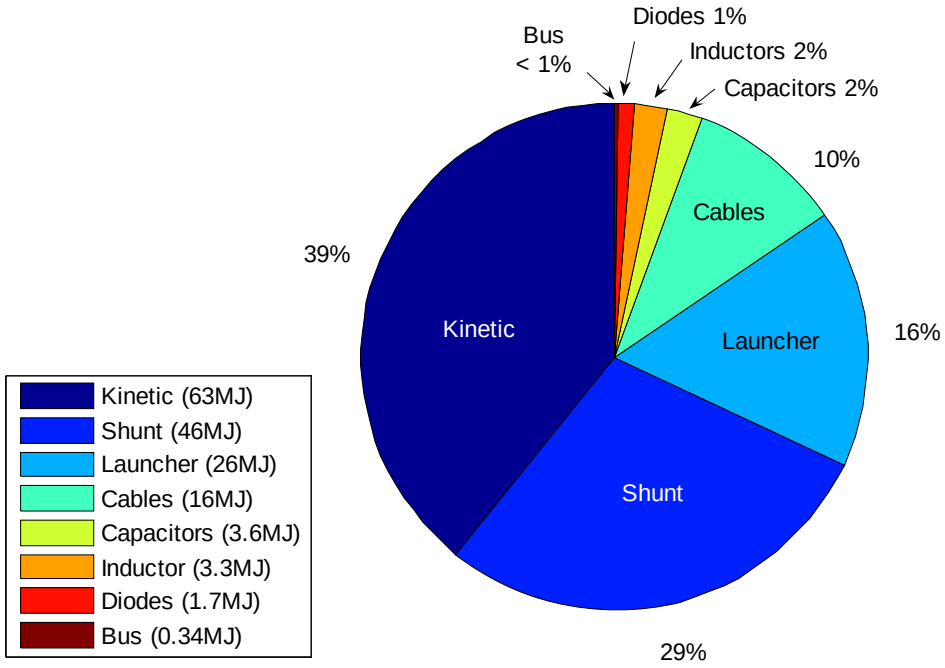

Figure 3. Energy distribution after a single shot using the parameters given in Table 1.

Once the heat generation is known for each component of the circuit, the change in the bulk temperature of each component can be calculated. It is assumed that each component is heated uniformly; however, localized temperature differences in the capacitor, thyristor, and diodes are expected and will limit the steady state operating temperatures of these devices. If the component is comprised of several materials, the mass fractions were used to determine a composite specific heat. Table 3 shows the energy deposited in an individual component and the component mass, specific heat, and change in temperature after a single shot. The maximum energy deposition per component came from the first bank of discharged modules, which deliver the highest currents. For the components that are only in the circuit while the capacitor is discharging, the heat load per component was fairly consistent across all of the banks. The inductor, cables and diode of a previous banks can be influence by the discharge of

subsequent capacitors, therefore the heat load was higher for these components the earlier the bank was discharged.

In order to calculate the surface heat flux reported in the last column of Table 2, the heat generation rate of each component was determined by taking the pulsed heat load and distributing that load over the time periods between pulses. The surface area of each component was then approximated based on a system that has been designed for a 32 MJ Launcher to be built at NSWC Dahlgren Division.

Table II. Thermal response of the individual components from a single shot.

Component	Energy Deposited* (kJ)	Mass (kg)	Specific Heat (J/kgK)	Temperature Change (°C)	Surface Heat Flux (kW/m^2)$^+$
Capacitor	3.48	140.2	1509	0.013	0.21
Inductor	102.1	350	414.5	0.7	11.2
Bus	8.0	46	903	0.19	0.16
Diode	1.88	2.8	385	2.21	9.9
Thyristor	1.63	2.9	385	3.28	10.4
Cables	8.2 kJ/m	2.7 kg/m	385	7.9	10.3

$^+$ based on 6 rounds per minute

* maximum energy deposited in a single component

The thermal mass of the capacitors and the bus bar will enable these devices to be fired a large number of times without any external cooling. Air cooling of the capacitor banks and the bus bar is a distinct possibility due to their high thermal mass and surface area. In the event that these systems are air cooled, they represent a significant heat generation rate of 724 kW that should not be dumped onto HVAC system without careful consideration. While the heating of these components should not adversely influence the system for several hundred shots, this heat must ultimately be removed by the HVAC system which represents a system inefficiency and fuel cost. It is conceivable that these systems could be designed such that their compartments could be cooled using external air in unconditioned spaces, although this may be difficult in a marine enviroment.

In the event that the system will maintain a sustained rate of fire for more than a few rounds; the inductor, diodes, thyristors, and cables will require an active cooling system. The surface heat flux shown is the very upper end of air cooling and would require complicated heat sinks and/or higher operating temperatures. In addition, unlike the capacitor bank this would represent an immediate heat load to the compartment that contains these devices. The cables are perhaps the easiest to air cool and the hardest to liquid cool due to their geometry, however they also represent a significant heat load.

The heat load of 1.6 MW calculated was based on 30 m long cables which could be reduced by using additional cables and shorter cables as necessary.

IV. CONCLUSIONS

A capacitor-based pulse-forming network has been modeled and transient behavior solved using a finite difference approach. Using this approach allowed the simulation to account for a large number of individually triggered capacitor banks and therefore a very smooth current profile. The solution of the circuit was coupled with a finite difference solution for the penetration of the magnetic field and resistive heating of the launcher. The individual resistance of the capacitors, inductors, thyristors, diodes, bus bar, cable and the muzzle shunt were included in the model so that the heat generation rate could be calculated for each component. Once the deposited energy was known the temperature rise of the individual components could then be calculated. It was evident that the thermal mass of the capacitor banks will allow them to be fired a large number of times even without a cooling system. The inductors, diode, thyristor and cables will likely require liquid cooling otherwise these systems will present a large transient load on the HVAC system.

V. REFERENCES

[1] J. MacFarland and I.R. McNab, "A long-range naval railgun", *IEEE Trans. Magn.*, vol. 39, pp.289-294, Jan. 2003.

[2] J.S. Bernardes, M.F. Stumborg and T.E. Jean, "Analysis of a capacitor- based pulsed-power system for driving long-range electromagnetic guns", *IEEE Trans. Magn.*, vol. 39, pp.486-490, Jan. 2003

[3] R.K. Pitman, R.L. Ellis and J.S. Bernardes, "Iterative transient model for railgun electromechanical performance", *12th Symposium on Electromagnetic Launch Technology*, Salt Lake City, UT, May 2004

[4] J.V. Parker, "Electromagnetic projectile acceleration utilizing distributed energy sources", *Journal of Applied Physics*, vol. 53, October 1982

[5] F. J. Deadrick, et al., "MAGRAC - A railgun simulation program", *IEEE Trans. Magn.*, vol. MAG-18, pp. 94-104, Jan. 1982.

[6] D.E. Johnson and D.P. Bauer, "The effect of rail resistance on railgun efficiency", *IEEE Trans. Magn.*, vol. 25, pp. 271-276, Jan. 1989.

[7] J.V. Parker, *Modeling rail resistance in EM launchers*, IAT.R0186, May 1999.

[8] A.N. Smith, R.L. Ellis, J.S. Bernardes and A.E. Zielinski, "Thermal management and resistive rail heating of a large-scale naval electromagnetic launcher", *IEEE Trans. Magn.*, vol. 41, pp. 235-240, Jan. 2005.

[9] S. Satapathy and H. Vanicek, “Energy partition in a conceptual naval railgun at two scales”, *Proceedings of the 2004 ASNE High Power Weapons Systems Conference,* Annapolis, MD, Dec. 2004.

[10] J.S. Bernardes, G.P. LaCava and M.J. Schrader, “Analysis of a railgun capacitor-muzzle-shunt energy recovery scheme”, *Conference Record of the 25th International Power Modulator Conference,* Hollywood, CA, June 2002.